# Doped Poly-Si/$SiO_x$ Passivating Contacts: Hydrogenation and Its Mechanisms

Thien N. Truong[1], Di Yan[1], Andres Cuevas[1], Daniel Macdonald[1] and Hieu T. Nguyen[1]

[1]*The Australian national University, Canberra, ACT 2601 Australia*

**Abstract:** Polycrystalline silicon (poly-Si) passivating-contact solar cells are predicted to replace the everyday solar technology in the market in the next few years, with some pilot lines in production now. However, the poly-Si films possess two limitations: (i) They absorb strongly light in the ultra-violet to blue region, resulting in relatively large parasitic loss when employed on the front side of a solar cell, and (ii) They often contain a high density of defects which can potentially affect the quality of poly-Si/SiOx passivating contacts and limit the conversion efficiency of solar cells. Therefore, reducing defect densities inside the poly-Si films and improving their optoelectronic performances are critical to the commercialization of this technology. Here, we examine different hydrogen treatments to reduce the defect concentration inside the doped poly-Si films and to improve the passivation quality of the poly-Si/SiOx stacks. We demonstrate significant improvements in the passivation quality (presented by an increase of the implied open circuit voltage) of both boron and phosphorus-doped poly-Si/SiOx stacks formed on both n and p-type silicon substrates, with either planar or textured surfaces. Furthermore, combining various characterization techniques, we unlock key optical and electrical properties of the passivating-contact structures, providing critical insights about the mechanisms of the hydrogenation processes.

**Introduction:** Beyond the Passivated Emitter and Rear Cell (PERC) crystalline silicon (c-Si) technology with potential commercial cell conversion efficiencies in the range of 21 - 24% [1], c-Si solar cells incorporating poly-Si/$SiO_x$ passivating contacts have attracted significant interest as one of the most promising pathways to overcome the efficiency limits of the PERC technology [2]–[5]. In general, poly-Si films often contain a high density of defects which may affect the passivating-contact performance and thus the conversion efficiency of solar cells. This stems from the fact that poly-Si films, formed by recrystallizing amorphous Si (a-Si) films via a high-temperature processing step, often contains both amorphous and crystalline phases. In the a-Si phase, each Si atom is surrounded by four other Si atoms whose bonds are stretched, twisted, or broken (known as dangling bonds). These bonds then create energy levels inside the material bandgap and are responsible for Shockley-Read-Hall (SRH) carrier recombination. One way to overcome this SRH recombination is to neutralize each defective bond inside the films with the addition of a hydrogen atom, that is, by performing a hydrogenation step after the formation of the poly-Si film. On the other hand, the benefits of hydrogenation processes are well-known for c-Si wafers and solar cells. Therefore, in principle, hydrogenation techniques could also be used to passivate defects within the doped poly-Si films themselves, in a similar manner to the c-Si substrates, hence improving the overall performance of doped poly-Si/$SiO_x$ passivating contacts.

This work investigates effective methods to reduce the defect concentration inside the doped poly-Si films and to improve the passivation quality of the doped poly-Si/$SiO_x$ stacks. We first study the structural and optoelectronic properties of the doped poly-Si/$SiO_x$ passivating contacts on different substrates. We then demonstrate that atomic hydrogen, supplied by a $SiN_x$:H or $AlO_x$:H capping layer, can be effectively driven in to passivate defects inside various types of poly-Si films, thus improving the quality of the passivating-contact structures. Finally, we elucidate the underlying mechanisms of various post-treatments of doped poly-Si/$SiO_x$, including $AlO_x$:H and/or $SiN_x$:H films followed by FGA, and FGA alone, by tracking the evolution of their optoelectronic properties after each process.

## Results and Analysis

### *A. Structural and optoelectronic properties*

Figure 1A shows a high-resolution transmission electron microscopy (TEM) image of the interface. The interfacial oxide film can be observed as a thin stripe of amorphous structure between the poly-Si and c-Si, as noted in the figure. The doped poly-Si layer shows both crystalline and amorphous phases,

whereas as expected, the c-Si substrate shows a very uniform crystalline structure. Figure 1B shows the evolution of the PL spectra from the phosphorus-doped poly-Si samples before and after hydrogenation. There is a clear PL peak associated with the a-Si:H content after hydrogenation, indicating that the atomic hydrogen in the $SiN_x$:H films has been driven into the doped poly-Si films [6]. Figure 1C shows a high-angle annular dark-field (HAADF) image of a vertical cross-section of one pyramid at the surface. The interfacial silicon oxide layer can be observed as a thin amorphous $SiO_x$ stripe in the TEM image (Figure 1C-1). However, there is a clear disruption of the oxide interface, and the thickness of the poly-Si film is ~40 nm. On the other hand, Figure 1C-2 shows a TEM image at the pyramid's peak area (area 2). The poly-Si film is thinner (~20 nm) and there are is no clear boundary between the poly-Si film and c-Si substrate. There is no feature that represents the amorphous phase of the $SiO_x$ interfacial layer either. Surprisingly, the luminescence properties of the stacks are remarkably different. There is no clear a-Si:H PL peak emitted from the phosphorus-doped poly-Si film after the hydrogen treatment on n-textured substrates (Figure 1D). Also, the phosphorus-doped poly-Si PL peak intensity is minimal, although it slightly increases after the treatment. We hypothesize that the disappearance of the a-Si:H PL peak and the minimal intensity of the poly-Si PL peak, after the hydrogenation treatment, on the textured substrate are due to the absence of the ultrathin oxide interface around the pyramid peaks and the oxide disruption on the pyramid sides. The oxide absence and disruption cause a lack of photoinduced carrier build-up inside the doped-poly film [7]. Note that, even with the oxide absence and disruption, the implied open circuit voltage ($iV_{oc}$) values are still >700 mV before and after hydrogenation. This could be due to the very small area of the disrupted and absent oxide regions compared to the normal oxide region. Moreover, Figure 1E shows FTIR results from the hydrogenated phosphorus-doped poly-Si sample at different stages: the poly-Si film is still present, only the film is removed by TMAH etching, and both the film and oxide layer are removed. The captured spectrum presents a clear stretching mode of Si− H bonds (1900~2200 $cm^{-1}$) in the sample with the hydrogenated poly-Si layer. When the layer is removed, the peak also disappears regardless of the presence of the oxide interface. This demonstrates that the amount of hydrogen in the poly-Si layer is still relatively high whereas that in the oxide interface is little or below the detection limit of our FTIR tool.

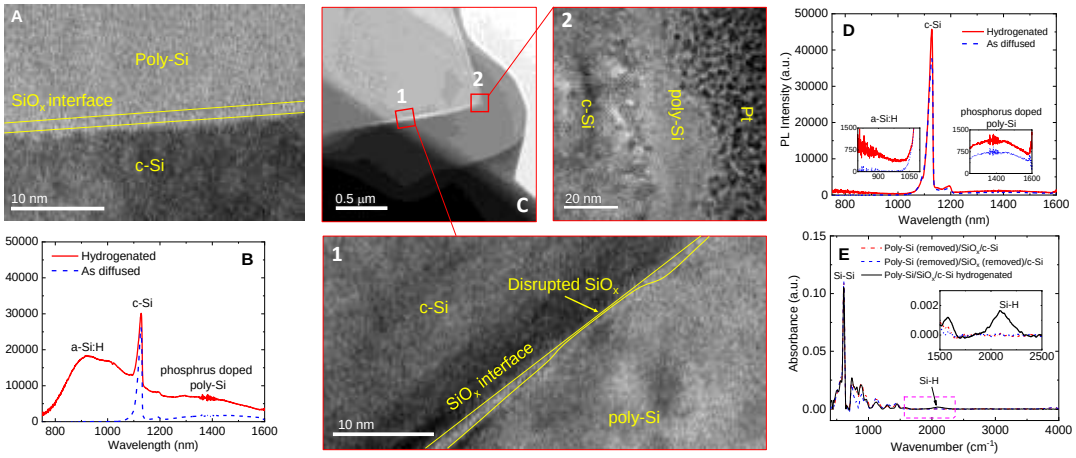


**Figure 1**. (A) High-resolution TEM image of an 830 °C phosphorus-doped poly-Si/$SiO_x$/c-Si structure on a planar substrate. (B) PL spectra captured from the sample before and after hydrogenation by $SiN_x$:H + FGA. (C) HAADF image of a vertical cross-section of a pyramid at the sample surface: (1) TEM image of the selected area at the edge and (2) at the peak of the pyramid. (D) PL spectra captured from the textured 830 °C phosphorus-diffused poly-Si/$SiO_x$/c-Si sample before and after hydrogenation. (E) FTIR absorbance spectra captured from a hydrogenated 830 °C phosphorus-doped poly-Si/$SiO_x$/c-Si sample with the poly-Si film present, and with the poly-Si film and/or $SiO_x$ layer removed. All PL measurements conducted using an excitation laser of 405 nm at 80 K.

### *B. Effects of hydrogen treatments on the performance of passivating contacts*

Figure 2A and 2B show a significant improvement in $iV_{oc}$ at 1-sun intensity from various planar phosphorus-doped poly-Si samples after a $SiN_x$:H assisted hydrogen treatment. All samples, initially with either low or high passivation qualities (some with <670 mV for n-type 1 Ω.cm c-Si substrates or some with >700 mV for p-type 100 Ω.cm c-Si substrates), have $iV_{oc}$ boosted. The improvement can also be observed for all investigated planar boron-doped poly-Si samples, as shown in Figure 2C and 2D. Figure 2E shows $iV_{oc}$ of phosphorus doped samples hydrogenated by thermal assisted atomic layer deposition (ALD) $AlO_x$:H + FGA, $SiN_x$:H + FGA, and FGA only. All samples after the phosphorus diffusion

show good initial passivation qualities ($iV_{oc}$ ~ 685–700 mV). Some of the phosphorus-doped poly-Si/$SiO_x$ samples were then annealed in forming gas at 400 °C for 30 min without any capping layer. The samples with a high resistivity (100 Ω.cm) showed a dramatic increment in $iV_{oc}$ values after the annealing ($\Delta iV_{oc}$ ~ 28 mV), whereas on low-resistivity samples (2 Ω.cm), the change was minimal. The other samples, annealed in forming gas in the presence of an $AlO_x$:H capping layer, showed a significant increment in iVoc values ($iV_{oc}$ > 725 mV) regardless of the initial conditions.

To compare the $AlO_x$:H + FGA and $SiN_x$:H + FGA hydrogen treatments, we continued capping the already hydrogenated samples (via FGA alone and $AlO_x$:H + FGA) with $SiN_x$:H films and subsequently annealed them in forming gas ($SiN_x$:H + FGA), as shown in Figure 2E. There was a slight reduction in the passivation quality of the samples initially hydrogenated by $AlO_x$:H + FGA (of both low- and high-resistivity substrates) but a significant improvement of samples initially hydrogenated by FGA only (especially low-resistivity substrates). The surface passivation reduction of the samples with pre-$AlO_x$:H + FGA after the second hydrogenation step by $SiN_x$:H + FGA (after having removed the $AlO_x$:H layer) could be due to two possible reasons. First, the hydrogenated poly-Si films may have been damaged by the plasma from the PECVD $SiN_x$:H deposition. Second, the samples may have been injected with too much hydrogen, which could cause a hydrogen-induced degradation. We can conclude that the former is the main reason for the decreasing passivation quality, as we subsequently injected even more hydrogen by a third hydrogenation step ($SiN_x$:H + FGA 2) but did not observe any passivation change. Despite that, $iV_{oc}$ values were all very high (715–727 mV) after the second hydrogenation step.

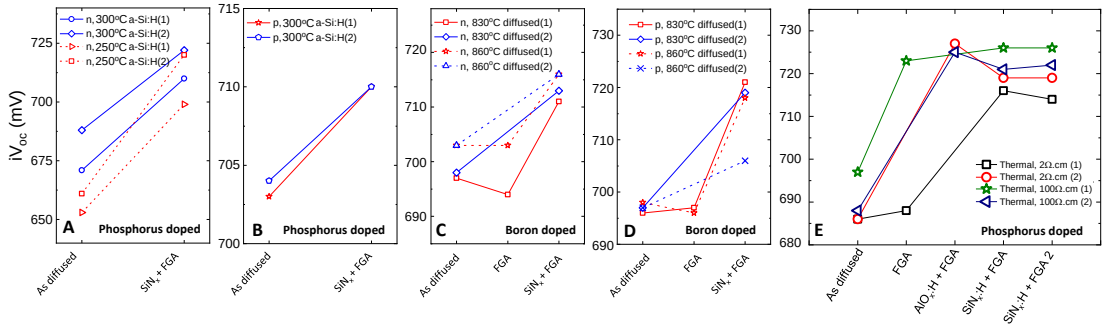


**Figure 2**. Implied open circuit voltages $iV_{oc}$ of various poly-Si/$SiO_x$/c-Si samples before and after different hydrogenation steps. The poly-Si films are doped with (A, B, E) phosphorus and (C, D) boron. The c-Si substrates are planar. (A) 1 Ω.cm n-type substrate, 250 °C and 300 °C deposition temperatures of a-Si:H films, 830 °C diffusion temperature to form poly-Si films. (B) 100 Ω.cm p-type substrate, 300 °C deposition temperatures of a-Si:H films, 830 °C diffusion temperature to form poly-Si films. (C) 1 Ω.cm n-type and (D) 100 Ω.cm p-type substrates, 300 °C deposition temperatures of a-Si:H films, 830 °C and 860 °C diffusion temperature to form poly-Si films. (E) Samples before and after various hydrogenation methods: FGA alone and $AlO_x$:H or $SiN_x$:H followed by FGA. The $iV_{oc}$ are measured at a 1-sun equivalent intensity.

### *C. Mechanisms of different hydrogen post-treatments*

Figure 3A presents the PL spectra captured from the poly-Si/$SiO_x$/c-Si sample at 80 K using the 405 nm excitation laser after various processing steps: as diffused and subsequently annealed in forming gas with and without the $AlO_x$:H capping layer. In all cases, the spectra are nearly identical. In contrast, it is known that the poly-Si films contain both amorphous and crystalline phases, and the hydrogenated a-Si (a-Si:H) phase will emit a distinct peak located at ~950 nm, as shown in Figure 1B [8]. Surprisingly, there is no PL peak from the a-Si:H phase after the $AlO_x$:H deposition and subsequent FGA (Figure 3A), albeit there being a big improvement in the passivation quality (Figure 2E). These results demonstrate that the 40 nm $AlO_x$:H film had injected some amount of atomic hydrogen into the sample, which sufficiently passivated defects at the $SiO_x$/c-Si or poly-Si/$SiO_x$ interfaces. However, the hydrogen had not neutralized the non-radiative defects inside the poly-Si films or the dangling bonds associated with the a-Si phase. Figure 3B shows the PL spectra captured from the samples after the second hydrogenation step ($SiN_x$:H + FGA) at 80 K. Compared to the as-diffused sample, the poly-Si PL intensity (FGA + ($SiN_x$:H + FGA)) also increases indicating that some non-radiative defects inside the poly-Si layer have been passivated. Interestingly, the PL spectrum from the sample with pre-$AlO_x$:H + FGA even shows a much more significant increment in the PL intensities of both a-Si:H and poly-Si ($AlO_x$:H + FGA + ($SiN_x$:H + FGA)). These results suggest that as more hydrogen is injected, more non-radiative defects inside the poly-Si films and their a-Si phase are passivated.

Figure 3C shows SIMS hydrogen profiles inside the doped poly-Si films after the different hydrogen treatments. After the hydrogen treatments, the profiles showed significant hydrogen in the poly-Si films. Surprisingly, similar hydrogen contents were observed for the $AlO_x$:H + FGA and FGA + ($SiN_x$:H + FGA) treated samples, although the former did not show any a-Si:H PL peak (Figure 3A), whereas the latter did (Figure 3B). We hypothesize that the two different capping layers, $AlO_x$:H and $SiN_x$:H, could cause different associations of hydrogen in the poly-Si films, as illustrated in Figure 3D. The hydrogen from the $AlO_x$:H film could be injected into the poly-Si film and form complexes with other species rather than passivate the dangling bonds of the a-Si phase. Meanwhile, the hydrogen atoms from the $SiN_x$:H film both passivate the a-Si phase and form complexes. Consequently, after the two-step treatment by ($AlO_x$:H + FGA) + ($SiN_x$:H + FGA), the hydrogen concentration increases compared to both types of single step (Figure 3C) and the a-Si:H PL peak also increases significantly. With the two-step treatment, more hydrogen from the second process ($SiN_x$:H + FGA) is available to passivate the a-Si dangling bonds as other species in the poly-Si film already formed complexes with the hydrogen from the first process ($AlO_x$:H + FGA).

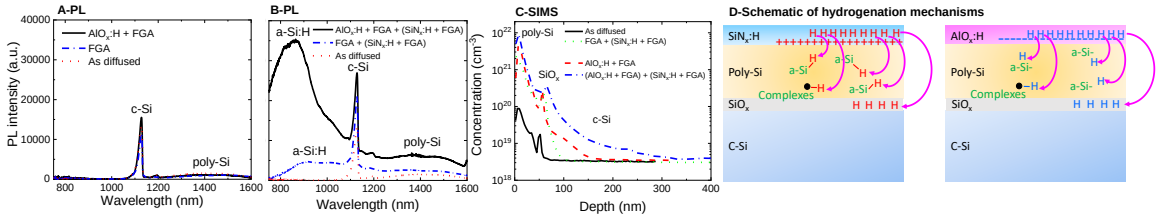


**Figure 3**. PL spectra captured from the phosphorus-doped poly-Si/$SiO_x$/c-Si samples after (A) thermal ALD $AlO_x$:H + FGA hydrogenation and (B) the subsequent $SiN_x$:H + FGA hydrogenation, using the 405 nm excitation laser at 80 K. (C) Hydrogen profiles by SIMS before and after different hydrogenation steps. (D) Schematic of the proposed hydrogenation mechanisms from different capping layers. The samples' substrate resistivity is 2 Ω.cm.

## Scientific innovation and relevance

Chasing a record efficiency of crystalline silicon (c-Si) solar cells is a relentless effort of the entire solar community. Upon that, poly-Si/$SiO_x$ passivating-contact solar cells are currently emerging as one of the most promising technologies. Significant effort has been placed on developing the contacts to achieve high-efficiency c-Si solar cells. The poly-Si film itself possesses some intrinsic limitations. To overcome that, hydrogen treatments have been chosen as methods to passivate defects inside the poly-Si film and interfaces. Our studies on the optoelectronic properties of the poly-Si/$SiO_x$ contacts and mechanisms of various hydrogen treatments on the contacts facilitate the development of high-efficiency c-Si solar cells. A range of applications stemmed from our studies are possible, including i) optimizing the dielectric layers to get the most effective hydrogenation, ii) investigating effects of different hydrogenation treatments on different poly-Si films and iii) incorporating the hydrogen treatments to the mass production of solar cells featuring poly-Si/$SiO_x$ passivating contacts.

## Conclusion

We have demonstrated the effectiveness of a hydrogenation treatment, via a capping hydrogen-rich silicon nitride or aluminum oxide films followed by a forming gas annealing step, for reducing defects inside poly-Si/$SiO_x$ passivating contacts. The treatment was found to improve the passivation quality (demonstrated by an increase of the implied open circuit voltage) of both boron and phosphorus-doped poly-Si/$SiO_x$ stacks formed on both n and p-type silicon substrates, with either planar or textured surfaces. We have also investigated the mechanisms of various post-treatment techniques of poly-Si/$SiO_x$ passivating contacts, including FGA, $AlO_x$:H + FGA, and $SiN_x$:H + FGA. Although all the treatment techniques investigated are effective, there are significant differences between them. For FGA, the performance depends on the substrates' resistivity. The captured PL spectra of the samples treated with FGA alone and those of the samples treated with $AlO_x$:H + FGA are identical to the captured PL spectra of the as-diffused sample (no a-Si:H PL peak and no). This demonstrates that only a very small amount of the injected hydrogen has been associated with the a-Si phase in the films, albeit a sufficient amount to passivate the interfaces, particularly in the case of $AlO_x$:H. However, after a subsequent second treatment step ($SiN_x$:H + FGA), the a-Si:H peak is revealed, demonstrating that hydrogen from the $SiN_x$:H film can passivate dangling bonds of the a-Si phase more effectively than hydrogen from the $AlO_x$:H film, even though in this study it did not result in a further improvement of the

interfaces. Our final presentation will provide more insights about the underlying mechanisms of these findings.

## References

[1] M. A. Green, “Photovoltaic technology and visions for the future,” *Prog. Energy*, vol. 1, no. 1, p. 013001, Jul. 2019.
[2] G. Yang *et al.*, “High-efficiency black IBC c-Si solar cells with poly-Si as carrier-selective passivating contacts,” *Sol. Energy Mater. Sol. Cells*, vol. 186, pp. 9–13, Nov. 2018.
[3] B. Nemeth *et al.*, “Polycrystalline silicon passivated tunneling contacts for high efficiency silicon solar cells,” *J. Mater. Res.*, vol. 31, no. 6, pp. 671–681, 2016.
[4] C. Messmer, A. Fell, F. Feldmann, N. Wohrle, J. Schon, and M. Hermle, “Efficiency Roadmap for Evolutionary Upgrades of PERC Solar Cells by TOPCon: Impact of Parasitic Absorption,” *IEEE J. Photovoltaics*, pp. 1–8, 2019.
[5] R. Peibst *et al.*, “For none, one, or two polarities—How do POLO junctions fit best into industrial Si solar cells?,” *Prog. Photovoltaics Res. Appl.*, no. September, pp. 1–14, 2019.
[6] T. N. Truong *et al.*, “Hydrogenation of Phosphorus-Doped Polycrystalline Silicon Films for Passivating Contact Solar Cells,” *ACS Appl. Mater. Interfaces*, vol. 11, no. 5, pp. 5554–5560, Feb. 2019.
[7] H. T. Nguyen *et al.*, “Sub-Bandgap Luminescence from Doped Polycrystalline and Amorphous Silicon Films and Its Application to Understanding Passivating-Contact Solar Cells,” *ACS Appl. Energy Mater.*, vol. 1, no. 11, pp. 6619–6625, Nov. 2018.
[8] T. N. Truong *et al.*, “Hydrogen-Assisted Defect Engineering of Doped Poly-Si Films for Passivating Contact Solar Cells,” *ACS Appl. Energy Mater.*, vol. 2, no. 12, pp. 8783–8791, Dec. 2019.